ANN Approach for Modeling of Mechanical Characteristics of RF MEMS Capacitive Switches - An Overview

Tomislav Ćirić[1], Zlatica Marinković[1], Olivera Pronić-Rančić[1], Vera Marković[1], Larissa Vietzorreck[2]

Abstract – **RF MEMS switches are nowadays based on a mature technology and are becoming a common component in the development of compact and tunable communication or measurement systems. The prediction of the switch performance is usually based on full-wave solvers in electromagnetic or mechanical domain or on using physically based models, where simplifications of the structure are done or some effects are neglected. In this paper, a comprehensive modeling methodology based on artificial neural networks (ANNs) will be shown. Different performance parameters or geometrical features of a device can be related by an ANN model. The model, once established, gives results in a much shorter time than standard simulators. It includes all effects considered in the numerical simulation or measurements it is based on. The derived model can be further used in system or circuit simulators. An overview of the ANN models in case of the mechanical characteristics of an electrostatically actuated capacitive RF MEMS switch, where the geometry parameters of a switch with complex shape and the actuation voltage are related, is given in this paper.**

Keywords – **RF MEMS, Artificial neural networks, Mechanical modeling, Actuation voltage, Capacitive switch.**

I. INTRODUCTION

RF MEMS components have been proven to be of great interest for RF circuits and subsystems, as they possess characteristics that may surpass conventional, purely electrical components. MEMS technology enables outstanding performance, compact design and tunability for a new generation of communication and measurement systems or sensor technology [1]. Key elements are switches and resonators as well as tunable varactors or inductors. For instance, RF MEMS switches convince with high linearity, low insertion loss and extremely good intermodulation performance. MEMS variable capacitors offer a higher Q-factor and wider tuning range than standard CMOS implementations. Moreover, its technology and architecture allows easy implementation in integrated circuits and therefore significantly reduces the size and weight of a system, for example a switch matrix for communication satellites, where the bulky mechanical switches can be replaced by much smaller RF MEMS switches [2].

In addition, the tunability brought by MEMS components can eliminate the need for hardware redundancy in an RF system.

However, even with the availability of more advanced simulation tools, the accurate simulation of RF MEMS components is still critical. In contrast to their electronic counterparts, the behavior of a micromechanical switch, for example, is determined by the coupling of electrical and mechanical, maybe even thermal properties, which makes the simulation much more complex while needing a multiphysics simulation approach.

Usually the basic simulations in the different physical domains are conducted by 3D numerical methods, like finite elements (FEM) or finite difference (FDTD) [3]-[7]. These methods are very general and offer accurate results, but due to technological features, like thin layers or small topological features, the calculation time and used memory is extensive. To overcome this problem, proper models have been developed, usually based on the physics of the component. For a single component they can give results quicker, what is extremely helpful for optimization procedures, where a series of simulations with varying parameters has to be run. On the other hand, models can be implemented into circuit simulators, connecting MEMS components with the other circuitry and enabling a mixed MEMS-IC co-simulation and systems simulations.

In order to get appropriate models, different approaches are followed. Analytical dependencies are used to simply describe the fundamental behavior of a component [8]. Mathematical-physical macro-models are derived for slightly simplified structures [9], e.g. to describe the mechanical dynamic behavior of a switch based on the energy balance [10]-[11]. Other approaches use libraries of lumped parametric elements, described by analytical or reduced-order models [12] like Coventor`s MEMS+ [13], which can be connected to more complex topologies for use in circuit simulators or even higher behavioral descriptions like Verilog A [14].

However, due to the simplifications involved in the description of the components or the lack of coupling and interaction between different parts of the topology, the results are usually less accurate and their prediction availability decreases.

In this paper, a different approach for RF MEMS switch modeling, the method based on using artificial neural networks (ANNs) [15], is considered. The modeling done here is not based on the physics of the structure, trying to simplify

Article history: Received December 01, 2016; Accepted June 03, 2017

[1]Tomislav Ćirić, Zlatica Marinković, Olivera Pronić-Rančić and Vera Marković are with the University of Niš, Faculty of Electronic Engineering, Aleksandra Medvedeva 14, 18000 Niš, Serbia, E-mails: cirict@live.com, zlatica.marinkovic@elfak.ni.ac.rs, olivera.pronic@elfak.ni.ac.rs, vera.markovic@elfak.ni.ac.rs

[2]Larissa Vietzorreck is with the TU München, Lehrstuhl für Hochfrequenztechnik, Arcisstr. 21, 80333 München, Germany, E-mail: vietzorreck@tum.de

the structure. Instead, a limited number of accurate numerical simulations are used to derive a behavioral model, relating e.g. geometrical or material parameters to electrical or mechanical properties like scattering parameters, resonance frequency or actuation voltage of an electrostatically activated MEMS switch [16]-[25]. The obtained models can provide accurate results for different characteristics in short time, considering all properties and coupling effects of the original complex structure and a wide range of the considered input quantities. In this paper, an overview of the ANN modeling methodology applications is given at the example of a coplanar capacitive electrostatically activated shunt switch [26]-[27], where the static mechanical behavior is modeled. In contrast to the work of other authors [16]-[19], a switch with a complex structure and shaped membrane is studied. Whereas in [20] and [22] only the electrical behavior has been described and single aspects of the mechanical modelling can be found in [23]-[24], in this contribution a comprehensive description about all aspects related to the mechanical model are given. The ANNs are applied in a direct approach to model the dependence of the necessary actuation voltage on the switch geometrical parameters. Moreover, for achieving the optimal switch performance, it is necessary to perform an optimization of the switch geometrical parameters (inverse modeling), which is usually done by numerous simulations for different values of the geometrical parameters or by applying time-consuming optimization procedures. In this paper ANN-based inverse models of the switch mechanical characteristics are also described. By using the ANN models the switch design procedure may become significantly shorter.

The paper is organized as follows. After Introduction, in Section II the considered capacitive RF MEMS switch is described. A short background on ANNs is given in Section III. The proposed procedures for direct and inverse modeling of RF MEMS switches are presented in Sections IV and V, respectively. Section VI contains the modeling results for both direct and inverse modeling approaches, a comparison with measured results and the corresponding discussions. Finally, the concluding remarks are given in Section VII.

II. Modeled Device

The analyzed structure is shown in Fig. 1. It is an electrostatically actuated CPW (Coplanar waveguide) capacitive shunt switch. It has been fabricated at the Fondazione Bruno Kessler (FBK) in Trento, Italy, in their established 8+ mask layer Silicon micromachining process [26]. On a HR Silicon wafer of 525 µm thickness with passivation of 1 µm SiO_2 the CPW is made by a 4 µm thick gold layer. The ground is connected by 1.8 µm thin gold membrane with a nominal gap size of 3 µm above the underpass, made by Aluminium/Titanium with 0.44 µm thickness. The underpass is covered by 0.1 µm SiO_2 to form the capacitive contact. In addition, a thin floating metal (Gold, 0.15 µm) is placed on top of the dielectric to ensure a good contact with the membrane in downstate. To activate the structure two DC actuation pads are placed next to the signal line, made by 0.63 µm thick Poly-Silicon covered by a 0.3 µm thin SiO_2. The actuation voltage is the minimum (pull-in) voltage (VPI) needed to move the bridge down. Its size is strongly determined by the geometry of the bridge (shape, length, thickness, gap), the mechanical parameters of the bridge material (Young modulus, Poisson's ratio) and the size and position of the actuation pads.

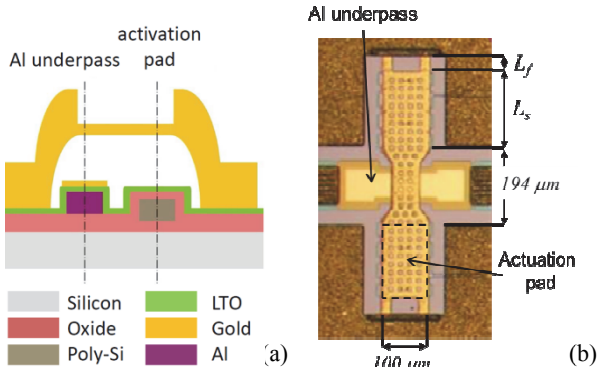

Fig. 1. (a) Schematic of the cross-section with 8+ layers in FBK technology and (b) top-view of the realized switch [26]

In the shown design the fixed-fixed beam bridge is anchored on both sides with two narrow fingers of 20 µm width and length L_f to make it more flexible and enable a lower actuation voltage V_{PI}. The middle part of the bridge is narrowed in order to form a defined capacitance with the signal line. The inductance of the bridge and the fixed capacitance between signal line and bridge form a series resonance, whose resonance frequency can be changed by varying the length of the fingered part, L_f, close to the anchors and the solid part, L_s. At series resonance the circuit acts as a short circuit to ground. Therefore, the bridge part lengths (L_f, L_s) should be carefully determined considering a feasible DC voltage supply by keeping the resonance at the desired frequency.

An analytic calculation for the actuation voltage is possible according to [1], if the spring constant k of the bridge is known. For simple bridge geometries like a rectangular bridge or a low-k bridge [28] (Fig. 2) approximate formulas to calculate the spring constants are given. Also, the perforation of the membrane can be taken into account by using a reduced value for the Young modulus. However, for a complex bridge shape the results deviate significantly from the much more exact numerical values, as can be seen in Fig. 3.

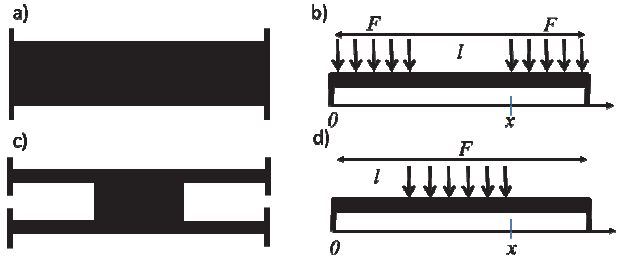

Fig. 2. (a) Simple rectangular shape of the membrane, used for analytic calculation, (b) assumed distribution of force, (c) low-k bridge shape with long fingers, (d) force distribution assumed for (c)

The closest agreement has been achieved with the model of the rectangular bridge, however, the flexible anchoring gives lower results than predicted and also the real distribution of actuation force, more centered in the middle, causes deviations. The given formulas for the fingered structure in Fig. 2c) were only valid with very long fingers and a central force, not applicable for the given geometry.

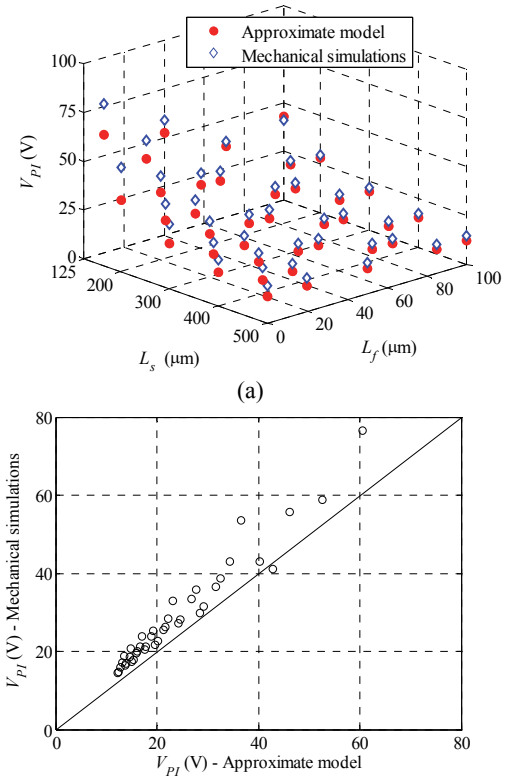

Fig. 3. Actuation voltage calculated by the approximate model versus simulations in the mechanical simulator [24]
(a) actuation voltage versus dimensions; (b) correlation plot

III. Artificial Neural Networks

The ANNs used in this work are multilayered ANNs [15]. A multilayered ANN consists of layers of neurons: an input layer, an output layer as well as one or more hidden layers. The number of neurons in the input layer equals to the number of independent input parameters, whereas the number of the output neurons equals to the number of parameters modeled by the ANN. Neurons within a layer are not interconnected, whereas each neuron is connected with all neurons from the next layer. As an illustration, in Fig. 4 ANNs with one and two hidden layers are shown. The ANNs have N neurons in the input layer, M neurons in the output layer, and H_1 and H_2 neurons in the first and second hidden layer, respectively. In this paper, the following notations of particular ANNs based on their structure are used: $N-H_1-M$ for a one hidden layer ANN and $N-H_1-H_2-M$ for a two hidden layer ANN. As an example, ANN denoted as 2-8-10-1 represents the ANN with two input neurons, eight and ten neurons in the first and second hidden layer, respectively, and one output neuron.

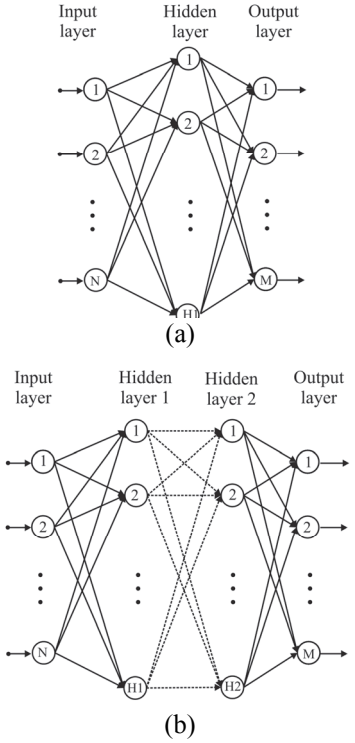

Fig. 4. Multilayered ANNs with
a) one hidden layer, b) two hidden layers.

Each neuron is characterised by an activation transfer function and each connection is weighted. The output of the l-th layer can be expressed as $\mathbf{Y}_l = F(\mathbf{W}_l\mathbf{Y}_{l-1} + \mathbf{B}_l)$, where $\mathbf{Y}_l$ and $\mathbf{Y}_{l-1}$ are outputs of the l-th and (l-1)-th layer, respectively, $\mathbf{W}_l$ is a weight matrix corresponding to the connections between the l-th and (l-1)-th layer, $\mathbf{B}_l$ is bias matrix of the l-th layer composed of the l-th layer neuron thresholds. Function F is the l-th layer transfer function (same for all neurons from a layer). In this case the input and output neurons have linear transfer functions, whereas the hidden neurons have a sigmoid transfer function (log-sigmoid function $F(u) = 1/(1+e^{-u})$ or tan-sigmoid function $F(u) = (e^{u} - e^{-u})/(e^{u} + e^{-u})$).

An ANN has ability to learn, i.e., to be train to predict the relationship among input and output parameters from the given sets of input-output data. The learning is achieved by adjustment of the parameters of the ANNs: thresholds of neurons and connection weights. For this purpose, several algorithms have been developed. One of the basic training algorithms is *backpropagation*algorithm, which can be briefly described as follows. Input to the procedure is the training set consisting of several combinations of input parameters and corresponding output targets. Although there are different approaches how to set the initial values of the ANN parameters, the initial values are commonly randomly set. The input vectors are presented to the input neurons and output vectors are computed. These output vectors are then compared with desired target values and errors are computed. Error derivatives are then calculated and summed up for each

weight and bias until whole training set has been presented to the network. These error derivatives are then used to update the weights and biases for neurons in the model. The training process proceeds until errors are lower than the prescribed values or until the maximum number of epochs (epoch - the whole training set processing) is reached. There are also modifications of this algorithm which have higher convergence order than the *backpropagation* algorithm, as *Levenberg-Marquardt* algorithm[15] which has been applied in this work.

The quality of the ANN learning and generalization is estimated by comparing the ANN outputs with the corresponding targets. Usually, average relative errors and maximum absolute errors are used as the measure of the ANN accuracy. Moreover, it is very convenient to use correlation coefficient which represents a measure of correlation of the simulated and target values, having maximum value 1, which indicates ideal modeling. The *Pearson product* correlation coefficient is used in this work [15]:

$$r = \frac{\sum (x_i - \bar{x})(y_i - \bar{y})}{\sqrt{\sum (x_i - \bar{x})^2 \sum (y_i - \bar{y})^2}}, \qquad (1)$$

where x_i and y_i are values of the desired target output and simulated output, respectively, in the *i*-th sample of the test set and $\bar{x}$ and $\bar{y}$ represent their mean values over the test set.

The number of hidden neurons of an ANN cannot be a priori set, therefore in order to find an optimal structure for the given size of input and output layers, ANNs with different number of hidden neurons are trained and tested for each considered input-output structure. After their assessment, the network with the best modeling results is chosen as the final neural model. This approach has been applied for all the models presented in this paper.

Once trained ANNs give correct response for different combinations of the input parameter values, no matter if they have been used for the model development or not. The ANN generalization, i.e., their ability to give the correct response for the input values not used for their training, qualified them as an efficient modeling tool in the field of RF and microwaves [15], [30]-[38]. Furthermore, as finding the ANN response assumes calculation of basic mathematical operations and exponential functions, the network response is calculated practically instantaneously, which also gives a significant advantage of the models based on ANNs.

IV. ANN Based Switch Actuation Voltage Modeling - Direct Approach

The direct approach to the ANN based switch actuation voltage modeling refers to development of the model consisting of an ANN trained to model the switch actuation voltage V_{PI} versus the considered switch geometrical parameters L_s and L_f as inputs, as shown in Fig. 5, [22]. This model will be named further as the direct model of the switch actuation voltage. The ANN has two input neurons corresponding to the two geometrical parameters and one output neuron corresponding to the actuation voltage. The ANNs are trained by using the values of the actuation voltage calculated in a mechanical simulator [39] for several combinations of the considered switch geometrical parameters. The model development procedure is illustrated in Fig. 6. Namely, as mentioned in the previous section, several ANNs with different number of hidden layers and hidden neurons are trained using the same training set. Once the ANN giving the best accuracy has been determined, this model can be further used for fast calculation of the actuation voltage for any combination of the geometrical parameters within the range spanned by the values of the training set.

Fig. 5. Direct ANN model of the RF MEMS switch actuation voltage

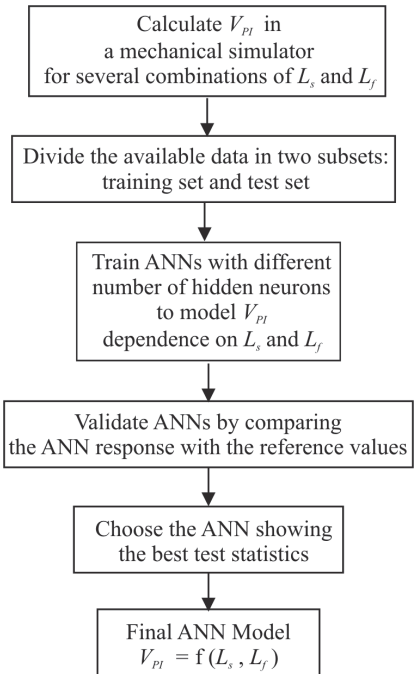

Fig. 6. Procedure for development of the direct ANN model of RF MEMS switch actuation voltage

V. ANN Based Switch Actuation Voltage Modeling - Inverse Approach

The direct model described above can be used for quick determination of the actuation voltage for the given values of the geometrical parameters. Also, it can be used to optimize one of the switch geometrical parameters in order to satisfy the desired value of the actuation voltage, making the optimization time significantly shorter comparing to the optimization in mechanical simulators. However, a need for the optimizations still remains.

Optimizations could be completely avoided by applying an ANN based approach for the switch inverse modeling. The idea is to exchange one input and output parameter and to train new ANNs to calculate one of the considered switch

dimensions (L_f or L_s) for the fixed value of the other dimension and the desired actuation voltage, as shown in Fig. 7 [22]. Each of these ANNs has two inputs and one output neuron.

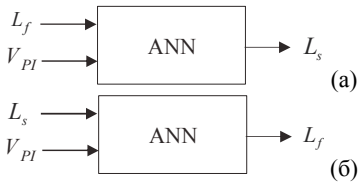

Fig. 7. Inverse ANN models of the RF MEMS switch actuation voltage: (a) solid part length determination; (b) fingered part length determination

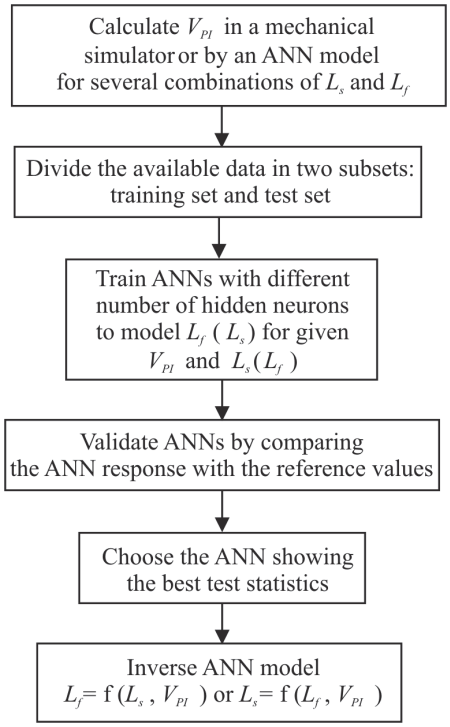

Fig. 8. Procedure for development of ANN models for inverse modeling of RF MEMS switches

For the training of such ANNs, as for the direct ANN model, it is necessary to acquire the corresponding simulated data, i.e. the actuation voltage calculated for several combinations of the switch geometrical parameters. The data can be obtained by using mechanical simulators. If it turns out that the number of combinations, necessary to obtain accurate results in the direct model, is not sufficient to give adequate results in the inverse model, more training data are needed. The extension of the training set with combinations calculated by the mechanical solver is time consuming, however, the already existent direct approach can be used to calculate new training samples in short time, as will be demonstrated within the section reporting the results.

The procedure of the inverse model development is illustrated in Fig. 8. An appropriate training set is developed from the available data, having one switch dimension and the calculated actuation voltage as inputs and the other dimension, which is to be determined, as the target output. Among the trained ANNs with different number of hidden layers and hidden neurons, the ANN giving the best validation characteristics is chosen as the final inverse model.

VI. Numerical Results

The described direct and inverse ANN models of the actuation voltage of the considered switch were developed for the switch depicted in Fig. 1 with the variable geometrical parameters falling in the following ranges: L_s from 50 μm to 500 μm, and L_f from 0 μm to 100 μm. For the model development, i.e., for training and validating ANNs, the actuation voltage V_{PI} was simulated for 39 combinations of the geometrical parameters L_f or L_s by COMSOL Multiphysics [39]. The distribution of the values of geometrical parameters followed mostly a uniform grid.

A. Direct Modeling

To develop the direct model described in Section IV, a training set containing 30 out of 39 data samples was used. The remaining nine data samples were used for ANN model validation. Among the several trained ANNs, the best results were achieved by the model (2-8-1), containing 8 neurons in the hidden layer. The high level of the ANN learning is proved by the correlation plot for the training set shown in Fig. 9.

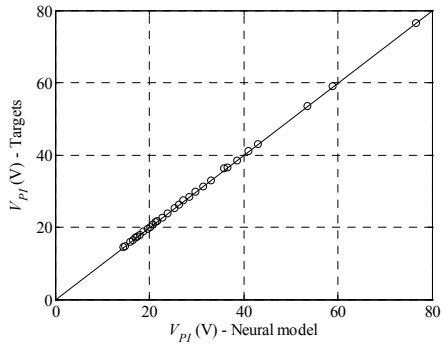

Fig. 9. Actuation voltage correlation plot for the training set

TABLE I
TEST RESULTS FOR THE DATA NOT USED DURING THE TRAINING

L_s (μm)	L_f (μm)	V_{PI}(target) (V)	V_{PI}(ANN) (V)	$\|\Delta V_{PI}\|$ (V)	$\|\Delta V_{PI}/V_{PI}\|$ (%)
150	25	55.6	55.58	0.02	0.01
150	65	43	43.45	0.45	1.10
250	25	33.3	33.16	0.14	0.40
250	65	28.2	28.21	0.01	0.03
350	10	25.2	25.32	0.12	0.47
350	25	23.8	23.74	0.06	0.25
350	65	21.1	20.99	0.11	0.54
350	75	20.5	20.45	0.35	0.17
450	65	16.9	16.80	0.10	0.57

TABLE II
ACTUATION VOLTAGE DEVIATION FOR L_s CHANGES

ΔL_S (μm)	Avg $\lvert\Delta V_{PI}\rvert$ (V)	Avg$\lvert\Delta V_{PI}/V_{PI}\rvert$ (%)	Max$\lvert\Delta V_{PI}\rvert$ (V)
L_s = 200 μm			
-10	1.9	4.9	3.1
-5	0.92	2.4	1.5
-4	0.73	1.9	1.2
-3	0.55	1.4	0.91
-2	0.36	0.94	0.6
-1	0.18	0.47	0.3
+1	0.18	0.46	0.3
+2	0.36	0.92	0.59
+3	0.53	1.4	0.89
+4	0.71	1.8	1.2
+5	0.88	2.3	1.5
+10	1.7	4.4	2.9
L_s = 300 μm			
-10	0.86	3.3	1.4
-5	0.42	1.6	0.68
-4	0.34	1.3	0.54
-3	0.25	0.97	0.41
-2	0.17	0.64	0.27
-1	0.083	0.32	0.13
+1	0.083	0.32	0.13
+2	0.17	0.64	0.27
+3	0.25	0.95	0.4
+4	0.33	1.3	0.53
+5	0.41	1.6	0.66
+10	0.81	3.1	1.3
L_s = 450 μm			
-10	0.38	2.1	0.43
-5	0.19	1.1	0.21
-4	0.15	0.86	0.17
-3	0.12	0.65	0.13
-2	0.078	0.43	0.087
-1	0.039	0.22	0.044
+1	0.039	0.22	0.044
+2	0.079	0.44	0.089
+3	0.12	0.66	0.13
+4	0.16	0.89	0.18
+5	0.2	1.1	0.23
+10	0.4	2.2	0.47

TABLE III
ACTUATION VOLTAGE DEVIATION FOR L_f CHANGES

ΔL_f (μm)	Avg $\lvert\Delta V_{PI}\rvert$ (V)	Avg$\lvert\Delta V_{PI} / V_{PI}\rvert$ (%)	Max$\lvert\Delta V_{PI}\rvert$ (V)
L_f = 20 μm			
-10	2.9	6.8	9.2
-5	1.3	3	4.5
-4	0.99	2.4	3.6
-3	0.73	1.7	2.6
-2	0.47	1.1	1.7
-1	0.23	0.56	0.84
+1	0.22	0.54	0.8
+2	0.43	1.1	1.6
+3	0.64	1.6	2.3
+4	0.83	2.1	3
+5	1	2.5	3.7
+10	1.9	4.8	6.6
L_f = 50 μm			
-10	1.4	4.2	4.4
-5	0.7	2.1	2.1
-4	0.56	1.6	1.7
-3	0.42	1.2	1.3
-2	0.28	0.81	0.85
-1	0.14	0.41	0.42
+1	0.14	0.4	0.42
+2	0.27	0.8	0.84
+3	0.41	1.2	1.3
+4	0.54	1.6	1.7
+5	0.67	2	2.1
+10	1.3	3.8	4.1
L_f = 80 μm			
-10	1	3.4	3.7
-5	0.51	1.6	1.8
-4	0.4	1.3	1.4
-3	0.3	0.98	1
-2	0.2	0.65	0.69
-1	0.099	0.32	0.34
+1	0.098	0.32	0.34
+2	0.19	0.63	0.67
+3	0.29	0.94	1
+4	0.38	1.3	1.3
+5	0.48	1.6	1.7
+10	0.93	3	3.2

In Table I, the test results for the validation test set consisting of nine samples not used for training are given: absolute deviation of the simulated actuation voltage values from the target ones $|\Delta V_{PI}|$ and relative error $|\Delta V_{PI} / V_{PI}|$ expressed in percent [22]. It can be seen that the maximum relative error is 1.1%. As these data were not used for the training, the results indicate a good generalization of the model.In order to evaluate the validity of the numerical simulations, the simulated actuation voltage is compared with the measured voltage for a realized structure. This component, fabricated at FBK in Trento, exhibits a finger length $L_f = 40$ μm and a length of the solid parts $L_s = 174$ μm. Different samples with the same dimensions have been thoroughly investigated regarding electrical and mechanical performance, long term behavior and temperature stability [40].

A plot of the actuation voltage measured at room temperature and higher temperatures is shown in Fig. 10. As the samples have been taken from different positions on the wafer, they exhibited small differences in the critical layer thicknesses of membrane and gap with a measured average gap size of 2.7μm. Therefore, the measured values for the actuation voltage vary in a certain range, however, the calculated actuation voltage, calculated for a structure with nominal gap size of 3 μm, is 44 V at room temperature, which is in good correspondence with the measurements.

Having in mind that the response of the ANN is instantaneous and that its accuracy is almost the same as the accuracy of the mechanical simulators, the developed model can be used further as an efficient tool for fast and accurate simulation of the actuation voltage of the considered switch. As an illustration, calculations necessary to make the plot

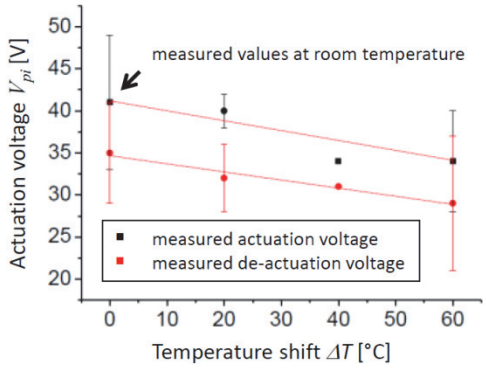

Fig. 10. Measured actuation voltage over temperature shift [40]

shown in Fig. 11 lasted only a few seconds, which is significantly faster than calculations in the mechanical simulator where a simulation of the actuation voltage lasts several tens of minutes per one combination of the bridge dimensions. High speed of the ANN model enables a comprehensive analysis of a switch, e.g. a sensitivity analysis investigating the influence of deviation of the geometrical parameters from their nominal values, caused by deviations in the manufacturing. Such an analysis is given in Tables II and III, for L_s and L_f, respectively. In both cases three fixed values of the geometrical parameter were considered (in lower, middle and higher part of their ranges) while the other parameters were changed over its range of values and the corresponding values of the actuation voltage were calculated. Then, for each of the three cases, the fixed parameter was changed up to +/-10 μm with the step of 1 μm, and the actuation voltages were calculated for the deviated value of the fixed parameter for all values of the second parameter. Average and maximum deviations from the desired actuation voltage values over the range of the second parameter were calculated for each changed value of the fixed parameters. The most illustrative values are given in Tables II and III. The results show that changes of actuation voltage have almost the same absolute value when one of the dimensions is increased or decreased for the same amount. Moreover, it is proved that the larger devices are more resistive to the fabrication deviations of the dimensions. For the considered technology the typical fabrication process tolerances are less then or in order of +/- 3 μm. Therefore, from the results given in the mentioned tables it can be seen that for that amount of the changes the actuation voltage changes are less than 1.5 %, which indicates that the deviation of the switch lateral dimensions during fabrication process has considerably small impact on the switch actuation voltage. Such a conclusion is confirmed by the results shown in Table IV, where the maximum deviations of the actuation voltage for simultaneous changes up to +/- 3 μm for several differently sized devices are given [23]. The maximum deviation of the actuation voltage is less than 2% (4 V in absolute values).

B. Inverse Modeling

First, the inverse RF MEMS switch models shown in Fig. 7, were developed by using the same training data as used for the development of the direct model described above (Training set 1). Although the trained ANNs learned well the training

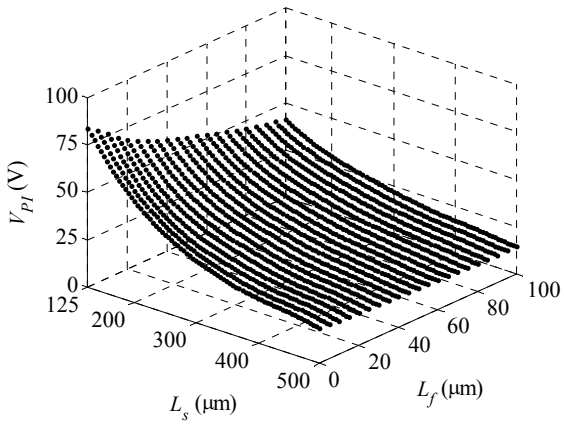

Fig. 11. Actuation voltage calculated by using the direct ANN model

TABLE IV
ACTUATION VOLTAGE CHANGES WITH SIMULTANEOUS CHANGES OF THE DIMENSIONS UP TO +/- 3 μm FOR DIFFERENTLY SIZED DEVICES

L_s (μm)	L_f (μm)	Max $\lvert\Delta V_{PI}\rvert$ (V)	Max $\lvert\Delta V_{PI}/V_{PI}\rvert$ (%)
200	20	1.7	3.9
200	50	1.1	3.1
200	80	0.76	2.4
300	20	0.61	2.1
300	50	0.51	2
300	80	0.43	1.9
450	20	0.38	1.9
450	50	0.31	1.8
450	80	0.18	1.1

data, the achieved generalization was unsatisfactory, because the relative errors on the test set not used for training were several tens of percent. For illustration, the test statistics for the best chosen ANNs (the ANNs (2-7-1) for L_f and (2-6-1) for L_s) can be seen in Tables V and VI. Increasing the number of hidden neurons and using two hidden layers led to even higher percentage errors on the test set caused by the ANN overlearning. This indicated that it was necessary to use more data for the training set. Building larger training sets assumes performing more time-consuming simulations. As illustration, for one combination of the considered geometrical parameters, simulation of the actuation voltage in a mechanical simulator lasts about two hours by using the computer in which a Quad-Core processor (2.83GHz) and 16GB RAMs are installed.

To avoid a further increase of time for the inverse model development, the direct ANN model described in the previous section was used to calculate more training sets in a short time. For the inverse model development of each parameter L_f or L_s, the modeling was started with the uniformly distributed training samples. Then, where the ANNs trained with the uniformly distributed values gave higher errors, the number of training samples was increased in the range of input values. The number of training samples was increased until the acceptable test error was achieved. The final training

TABLE V
INVERSE MODELING STATISTICS FOR THE TEST SET NOT USED FOR TRAINING: L_f

			Model (2-6-1)*			Model (2-25-25-1)**		
L_s (μm)	V_{PI} (V)	L_f(target) (μm)	L_f(ANN) (μm)	Abs. error (μm)	Relative error (%)	L_f(ANN) (μm)	Abs. error (μm)	Relative error (%)
150	55.6	25	29.26	4.26	17	24.87	0.13	0.5
150	43	65	66.44	1.44	2.2	66.73	1.73	2.7
250	33.3	25	21.36	3.64	15	24.28	0.72	2.9
250	28.2	65	62.65	2.35	3.6	65.06	0.06	0.1
350	25.2	10	11.57	1.57	16	11.19	1.19	12.0
350	23.8	25	27.94	2.94	12	23.99	1.01	4.1
350	21.1	65	67.78	2.78	4.3	62.73	2.27	3.5
350	20.5	75	77.72	2.72	3.6	74.38	0.62	0.8
450	16.9	65	64.25	0.75	1.2	62.47	2.53	3.9

*Training set 1: 30 samples obtained in the mechanical simulator and used for the direct model development
**Training set 2: 961 samples obtained by using the direct model

TABLE VI
INVERSE MODELING STATISTICS FOR THE TEST SET NOT USED FOR TRAINING: L_s

			Model (2-7-1)*			Model (2-4-6-1)**		
L_f (μm)	V_{PI} (V)	L_S(target) (μm)	L_S (ANN) (μm)	Abs. error (μm)	Relative error (%)	L_S(ANN) (μm)	Abs. error (μm)	Relative error (%)
25	55.6	150	167.84	17.84	12	150.10	0.10	0.1
65	43	150	153.13	3.13	2.1	151.65	1.65	1.1
25	33.3	250	252.05	2.05	0.8	250.24	0.24	0.1
65	28.2	250	250.50	0.50	0.2	250.16	0.16	0.1
10	25.2	350	350.75	0.75	0.2	350.03	0.03	0.01
25	23.8	350	346.32	3.68	1.1	347.44	2.56	0.7
65	21.1	350	347.82	2.18	0.6	348.09	1.91	0.5
75	20.5	350	347.69	2.31	0.6	349.12	0.88	0.2
65	16.9	450	453.80	3.80	0.8	447.98	2.02	0.4

*Training set 1: 30 samples obtained in the mechanical simulator and used for the direct model development
**Training set 2: 961 samples obtained by using the direct model

sets had 961 samples (Training set 2) including data corresponding to the combinations of the geometrical parameters from the original training set.

ANNs with one and two hidden layers were trained for both parameters. Among the trained ANNs with different numbers of hidden neurons, the following two ANNs were chosen as the final inverse model of the considered switch: (2-25-25-1) for L_f and (2-4-6-1) for L_s.

The test statistics on the validation test set not used for the model development were given in Tables V and VI. It can be seen that the relative errors are in most cases less than 4% for L_f and less than 1% for L_s. The absolute difference between predicted and expected values is less than 2.6 μm, which is close to fabrication tolerances, confirming the accuracy of the developed models.

The inverse models enable fast determination of the switch dimensions for the given actuation voltage. However, one have to take care about the input combinations, having in mind that every input combination will produce an output value, but not all combinations are physically possible. Therefore, before choosing an input combination, one should check if that combination is physically meaningful, which could be easily checked from the plots shown in Fig. 12. As an example, if Lf is to be determined for the actuation voltage of 40 V, L_s could not be higher than 250 μm approximately.

The question to develop a model which would predict both dimensions just from a given value of the activation voltage could be raised. Such a model could not be developed because this is not a unique mapping, meaning that a single value of the actuation voltage refers to several different combinations of the considered geometrical parameters.

VII. CONCLUSION

In this paper a modeling methodology for RF MEMS switches based on neural approaches has been shown. It has been started from the neural model aimed to predict the switch actuation voltage versus two lateral dimensions of the switch bridge. A direct model has been developed by using the actuation voltage values calculated by a mechanical simulator. Test results on the validation test set not used for the ANN training have shown that the model is able to accurately predict the actuation voltage for the given dimensions. The necessary calculation times are very short. Further, an efficient procedure based on ANNs aimed for finding the

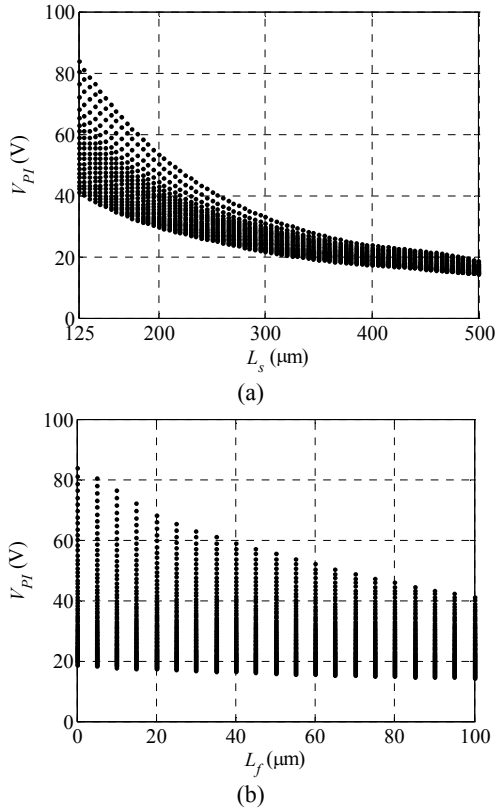

Fig. 12. Actuation voltage versus the bridge membrane dimensions: (a) solid part length, (b) fingered part length

optimal values of the switch geometrical parameters has been proposed in order to make time from the initial design to production even shorter. Namely, ANNs have been trained to predict one of two considered lateral dimensions for fixed other dimension and the given value of the actuation voltage. To develop inverse models in an efficient way, the fast computed data generated by the direct ANN models can be used in addition to those generated by the mechanical simulator. By using such inverse models, the switch geometrical parameters are determined instantaneously without time-consuming optimizations or numerous simulations in the simulators.

Although in the given example only the mechanical behavior dependent on some lateral dimensions of the switch is considered, the other geometrical parameters, as the bridge height, could be involved as well. In addition, the authors have previously developed the electrical models, direct and indirect, where the dependency between electrical properties like scattering parameters and geometry is taken into account. They could be combined with the mechanical ones shown here. Moreover, additional models could involve the temperature behavior as well. In that way a complete multi-physical description of the components could be created. The efficiency of this approach might not be obvious for a single switch development, as the model generation requires a couple of numerical simulations, which could be directly used to optimize or simulate the single switch. However, the necessary simulations can be run automatically for a parameterized model. On the other hand, for a mature technology, where numbers of switches with slight variations have to be produced meeting different requirements, this method can work as a very useful tool, speeding up the time for design and avoiding the use of different complex simulation tools.

ACKNOWLEDGEMENT

Authors would like to thank FBK Trento, Thales Alenia Italy, CNR Rome and University of Perugia, Italy for providing RF MEMS data and T.Kim for mechanical calculations. This work was funded by the bilateral Serbian-German project "Smart Modeling and Optimization of 3D Structured RF Components" supported by the DAAD foundation and Serbian Ministry of Education, Science and Technological Development. The work was also supported by the projects TR-32052 and III43012 of the Serbian Ministry of Education, Science and Technological Development.

REFERENCES

[1] G. M. Rebeiz, *RF MEMS Theory, Design, and Technology*, New York, Wiley, 2003.

[2] F. Diaferia, F. Deborgies, S. Di Nardo, B. Espana, P. Farinelli, A. Lucibello, R. Marcelli, B. Margesin, F. Giacomozzi, L. Vietzorreck and F. Vitulli, "Compact 12×12 Switch Matrix Integrating RF MEMS Switches in LTCC Hermetic Packages", *44th European Microwave Conference*, pp. 199-202, 2014.

[3] E. Hamad and A. Omar, "An Improved Two-Dimensional Coupled Electrostatic-Mechanical Model for RF MEMS Switches", *J. Micromech. Microeng*., vol. 16, no. 7, pp. 1424-1429, 2006.

[4] L. Vietzorreck, "EM Modeling of RF MEMS", *7th International Conference on Thermal, Mechanical and Multiphysics Simulation and Experiments in Micro-Electronics and Micro-Systems*, *EuroSime*, pp. 1-4, Como, Italy, 2006.

[5] Z. J. Guo, N. E. McGruer and G. G. Adams, "Modeling, Simulation and Measurement of the Dynamic Performance of an Ohmic Contact, Electrostatically Actuated RF MEMS Switch", *J. Micromech. Microeng*, vol. 17, pp. 1899-1909, 2007.

[6] R. Marcelli, A. Lucibello, G. De Angelis, E. Proietti, "Mechanical Modelling of Capacitive RF MEMS Shunt Switches", *Symposium on Test, Integration & Packaging of MEMS/MOEMS,* MEMS/MOEMS '09, pp. 19 -22, 2009.

[7] J. Bielen, and J. Stulemeijer, "Efficient Electrostatic-Mechanical Modeling of C-V Curves of RF-MEMS Switches", *International Conference on Thermal, Mechanical and Multi-Physics Simulation Experiments in Microelectronics and Micro-Systems, EuroSime 2007*, pp. 1-6, 2007.

[8] V. S. Cortes and G. Fischer, "Shunt MEMS Switch Requirements for Tunable Matching Network at 1.9 GHz in Composite Substrates", *German Microwave Conference (GeMiC 2015)*, Erlangen-Nurembeg, Germany, pp. 422-425, 2015.

[9] M. Niesner, G. Schrag, J. Iannucci and G. Wachutka, "Macromodel-Based Simulation and Measurement of the Dynamic Pull-in of Viscously Damped RF-MEMS Switches", *Sensors and Actuators A* 172, pp. 269-279, 2011.

[10] P. Heeb, W. Tschanun and R. Buser, "Fully Parameterized Model of a Voltage-Driven Capacitive Coupled Micromachinedohmic Contact Switch for RF Applications", *J. Micromech. Microeng*., vol. 22, no. 3, 2012.

[11] J. Casals-Terre, M. A. Llamas, D. Girbau, L. Pradell, A. Lazaro, F. Giacomozzi and S. Colpo, "Analytical Energy Model for the Dynamic Behavior of RF MEMS Switches Under Increased Actuation Voltage", *Journal of Microelectromechanical Systems*, vol. 23, no. 6, pp. 1428-1439, 2014.

[12] J. Iannacci, R. Gaddi and A. Gnudi, "A Experimental Validation of Mixed Electromechanical and Electromagnetic Modeling of RF-MEMS Devices Within a Standard IC Simulation Environment", *Journal of Microelectromechanical Systems*, vol. 19, no. 3, pp. 526-537, 2010.

[13] http://www.coventor/mems-solutions/products/mems

[14] D. Podoskin, K. Bruckner, M. Fischer, S. Gropp, D. Krausse, J. Nowak, M. Hoffmann, J. Muller, R. Sommer and M.A. Hein, "Multi-Technology Design of an Integrated MEMS-Based RF Oscillator Using a Novel Silicon-Ceramic Compound Substrate", *German Microwave Conference (GeMiC 2015)*, Erlangen-Nurembeg, Germany, March 16-18, pp. 406-409, 2015.

[15] Q. J. Zhang and K. C. Gupta, *Neural Networks for RF and Microwave Design*. Boston, MA: Artech House, 2000.

[16] Y. Lee, D. S. Filipovic, "Combined Full-Wave/ANN Based Modelling of MEMS Switches for RF and Microwave Applications", *IEEE Antennas and Propagation Society International Symposium*, vol. 1A, pp. 85-88, July 2005.

[17] Y. Mafinejad, A. Z. Kouzani and K. Mafinezhad, "Determining RF MEMS Switch Parameter by Neural Networks", *IEEE Region 10 Conference TENCON 2009*, pp. 1-5, 2009.

[18] Y. Lee, Y Park, F. Niu and D. Filipovic, "Artificial Neural Network Based Macromodeling Approach for Two-Port RF MEMS Resonating Structures", *IEEE Proceedings of Networking, Sensing and Control*, pp. 261-266, March 2005.

[19] Y. Gong, F. Zhao, H. Xin, J. Lin and Q. Bai, "Simulation and Optimal Design for RF MEMS Cantilevered Beam Switch", *International Conference on Future Computer and Communication* (FCC '09), pp. 84-87, June 2009.

[20] T. Kim, Z. Marinković, V. Marković, M. Milijić, O. Pronić-Rančić and L. Vietzorreck, "Efficient Modelling of an RF MEMS Capacitive Shunt Switch with Artificial Neural Networks", *URSI-B 2013 International Symposium on Electromagnetic Theory*, pp. 550-553, Hiroshima, Japan, 2013.

[21] L. Vietzorreck, M. Milijić, Z. Marinković, T. Kim, V. Marković and O. Pronić-Rančić, "Artificial Neural Networks for Efficient RF MEMS Modelling", *XXXI URSI General Assembly and Scientific Symposium (URSI GASS)*, pp 1-3, Beijing, China, 2014.

[22] Z. Marinković, T. Ćirić, T. Kim, L. Vietzorreck, O. Pronić-Rančić, M. Milijić and V. Marković, "ANN Based Inverse Modeling of RF MEMS Capacitive Switches", *11th Conf. on Telecommunications in Modern Satellite, Cable and Broadcasting Services - TELSIKS 2013*, pp. 366-369, Niš, Serbia, 2013.

[23] T. Ćirić, Z. Marinković, O. Pronić-Rančić, V. Marković and L. Vietzorreck, "ANN Approach for Analysis of Actuation Voltage Behavior of RF MEMS Capacitive Switches", *12th Intern. Conf. on Advanced Technologies, Systems and Services in Telecommunications - TELSIKS 2015*, pp. 381-384, Niš, Serbia, Sept. 14-17, 2015.

[24] Z. Marinković, A. Aleksić, T. Ćirić, O.Pronić-Rančić, V. Marković and T. Ćirić, "Analysis of RF MEMS Capacitive Switches by Using Neural Model of Actuation Voltage", *2nd Intern. Conf. on Electrical, Electronic and Computing Engineering - IcETRAN 2015*, pp. MTI2.3.1-5, Silver Lake, Serbia, June 8-11, 2015.

[25] Z. Marinković, V. Marković, T. Ćirić, L. Vietzorreck and O. Pronić-Rančić, "Artifical Neural Networks in RF MEMS Switch Modelling", *Facta Universitatis, Series: Electronics and Energetics*, vol. 29, no 2, pp. 177-191, 2016.

[26] S. DiNardo, P. Farinelli, F. Giacomozzi, G. Mannocchi, R. Marcelli , B. Margesin, P. Mezzanotte, V. Mulloni, P. Russer, R. Sorrentino, F. Vitulli and L. Vietzorreck, "Broadband RF-MEMS based SPDT", *European Microwave Conference 2006, Manchester*, Great Britain, September 2006.

[27] W. M. van Spengen, "Capacitive RF MEMS Switch Dielectric Charging and Reliability: a Critical Review with Recommendations", *J. Micromech. Microeng*., vol. 22, no. 7, 074001, 2012.

[28] R. J. Roark and W. C. Young, *Formulas for Stress and Strain*, 6th edition, McGraw-Hill, New York, 1989.

[29] F. Giannini, G. Leuzzi, G. Orengo and M. Albertini, "Small-Signal and Large-Signal Modeling of Active Devices Using CAD-Optimized Neural Networks", *Int. J. RF Microw. Comput.-Aided Eng.,* vol. 12, pp. 71-78, Jan 2002.

[30] J. E. Rayas-Sanchez, "EM-Based Optimization of Microwave Circuits Using ANN: The State-of-the-art," *IEEE Trans. Microw.Theory Tech.*, vol. 52, no. 1, pp. 420–435, 2004.

[31] A. Caddemi, F. Catalfamo and N. Donato, "Cryogenic HEMT Noise Modeling by Artificial Neural Networks", *Fluctuations and Noise Letters*, vol. 5, no. 3, pp. L423-L433, 2005.

[32] H. Taher, D. Schreurs and B. Nauwelaers, "Constitutive Relations for Nonlinear Modeling of Si/SiGe HBTs Using an ANN Model", *Int. J. RF Microw. Comput.-Aided Eng.*, vol. 15, no. 2, pp. 203-209, March 2005.

[33] Z. Marinković and V. Marković, "Temperature Dependent Models of Low-Noise Microwave Transistors Based on Neural Networks", *Int. J. RF Microw. Comput.-Aided Eng.*, vol. 15, no. 6, pp. 567-577, Nov. 2005.

[34] Z. Marinković, O. Pronić and V. Marković, "Bias-Dependent Scalable Modelling of Microwave FETs Based on Artificial Neural Networks", *Microw. Opt. Techn. Lett.*, vol. 48, no.10, pp. 1932-1936, Oct. 2006.

[35] H. Kabir, L. Zhang, M. Yu, P. Aaen, J. Wood and Q. J. Zhang, "Smart Modeling of Microwave Devices", *IEEE Microw. Mag.*, vol. 11, pp. 105–108, May 2010.

[36] Z. Marinković, G. Crupi, A. Caddemi and V. Marković, "Comparison Between Analytical and Neural Approaches for Multibias Small Signal Modeling of Microwave Scaled FETs", *Microw. Opt. Techn. Lett.*, vol. 52, no. 10, pp. 2238-2244, 2010.

[37] Z. Marinković, G. Crupi, D. M. M.-P. Schreurs, A. Caddemi and V. Marković, "Microwave FinFETModeling Based on Artificial Neural Networks Including Lossy Silicon Substrate", *Microelectron Eng.,* vol. 88, no. 10, pp. 3158-3163, 2011.

[38] Z. Marinković, O. Pronić-Rančić and V. Marković, "Small-Signal and Noise Modelling of Class of HEMTs Using Knowledge-Based Artificial Neural Networks", *Int. J. RF Microw. Comput.-Aided Eng.*, vol. 23, no. 1, pp. 34-39, January 2013.

[39] *COMSOL Multiphysics 4.3*, COMSOL, Inc.

[40] M. Barbato, A. Cester, V. Mulloni, B. Margesin, G. De Pasquale, A. Soma and G. Meneghesso, "Reliability of Capacitive RF MEMS Switches Subjected to Repetitive Impact Cycles at Different Temperatures", *44th European Solid State Device Research Conference (ESSDERC)*, pp. 70-73, Venice, Italy, Sept. 22-26, 2014.